Available online at www.sciencedirect.com
ScienceDirect
International Journal of Heat and Mass Transfer 50 (2007) 1963–1970
International Journal of HEAT and MASS TRANSFER
www.elsevier.com/locate/ijhmt

Thermal performance of plate-fin heat sinks under confined impinging jet conditions

Hung-Yi Li *, Kuan-Ying Chen

Department of Mechatronic Engineering, Huafan University, Shihtin, Taipei 22305, Taiwan, ROC

Received 8 June 2006; received in revised form 29 September 2006
Available online 29 November 2006

Abstract

This paper utilizes the infrared thermography technique to investigate the thermal performance of plate-fin heat sinks under confined impinging jet conditions. The parameters in this study include the Reynolds number (Re), the impingement distance (Y/D), the width (W/L) and the height (H/L) of the fins, which cover the range $Re = 5000$–$25{,}000$, $Y/D = 4$–28, $W/L = 0.08125$–0.15625 and $H/L = 0.375$–0.625. The influences of these parameters on the thermal performance of the plate-fin heat sinks are discussed. The experimental results show that the thermal resistance of the heat sink apparently decreases as the Reynolds number increases; however, the decreasing rate of the thermal resistance declines with the increase of the Reynolds number. An appropriate impingement distance can decrease the thermal resistance effectively, and the optimal impingement distance is increased as the Reynolds number increases. Moreover, the influence of the impingement distance on the thermal resistance at high Reynolds numbers becomes less conspicuous because the magnitude of the thermal resistance decreases with the Reynolds number. An increase of the fin width reduces the thermal resistance initially. Nevertheless, the thermal resistance rises sharply when the fin width is larger than a certain value. Increasing the fin height can increase the heat transfer area which lowers the thermal resistance. Moreover, the influence of the fin height on the thermal resistance seems less obvious than that of the fin width. To sum up all experimental results, Reynolds number $Re = 20{,}000$, impingement distant $Y/D = 16$, fin width $W/L = 0.1375$, and fin height $H/L = 0.625$ are the suggested parameters in this study.

Keywords: Confined impingement cooling; Plate-fin heat sink; Thermal resistance; Infrared thermography

1. Introduction

The operating capability and consumption power of electronic components have been increasing owing to the rapid development of the semiconductor technology. Inevitably the heat fluxes of the electronic components apparently rise because of the demands of powerful and miniature products. To remove heat efficiently from the high density electronic components becomes a crucial issue. Various cooling techniques, e.g. phase-change cooling, thermoelectric cooling, liquid cooling and impinging jet cooling, have been established to solve the problem. Impinging jet cooling combined with a heat sink provides a qualified solution for its direct, quick and local cooling characteristics. This cooling method has been investigated by a number of studies. Ledezma et al. [1] were concerned with the optimization of the heat transfer from pin fins under impinging air flow; they expressed the correlations for optimal fin-to-fin spacing and maximum thermal conductance. Sathe et al. [2] investigated the fluid motion and heat transfer from a pin-fin heat sink under an impinging flow; their simulations and experiments of the local temperatures showed similar results for the central part of the heat sink, but simulations overpredicted the temperatures around the outer edge of the heat sink base. The results indicated that the temperature of the substrate was low directly under the nozzle and it increased in the outward direction. Brignoni and Garimella [3] focused on

* Corresponding author. Tel.: +886 2 26632102x4017; fax: +886 2 26632102x4013.
E-mail address: hyli@huafan.hfu.edu.tw (H.-Y. Li).

0017-9310/$ - see front matter © 2006 Elsevier Ltd. All rights reserved.
doi:10.1016/j.ijheatmasstransfer.2006.09.024

Nomenclature

A	cross-sectional area of the heating element (mm^2)	R_{th}	thermal resistance (°C/W)
A_t	heat transfer area (mm^2)	T_{ave}	average temperature of the base of the heat sink (°C)
b	thickness of the base of the heat sink (mm)	T_l	temperature of the lower thermocouple in the heating element (°C)
D	nozzle diameter (mm)	T_u	temperature of the upper thermocouple in the heating element (°C)
d	distance between the two thermocouples in the heating element (mm)	T_∞	temperature of the impinging jet (°C)
G	inter-fin spacing (mm)	U	overall heat transfer coefficient (W/°C mm^2)
H	fin height (mm)	V	jet velocity (m/s)
k_{al}	thermal conductivity of aluminum alloy (W/mK)	W	fin width (mm)
L	length of the base of the heat sink (mm)	Y	impingement distance (mm)
n	fin number		
Q	heating power (W)	*Greek symbol*	
Re	Reynolds number	v	kinematic viscosity (m^2/s)

the heat transfer of a confined jet flow impinging on a pin-fin heat sink; with a fixed nozzle-to-target spacing, these workers varied the flow speed, diameter of nozzle and nozzle arrays and found that at a fixed air flow rate a nozzle of smaller diameter increased the impinging velocity and decreased the thermal resistance. Maveety and Hendricks [4] studied the influence of the geometry, the impingement distance, the material and the Reynolds number on the performance of pin-fin heat sinks with impingement cooling. The experimental results revealed that the fin geometry had an appreciable effect on the thermal resistance. The best thermal performance occurred when the dimensionless impingement distance was between 8 and 12. Moreover, the influence of the impingement distance on the performance was reduced as the Reynolds number was increased. Maveety and Jung [5] investigated the cooling performance of a pin-fin heat sink with air impingement flow; their simulations demonstrated a complicated fluid motion inside the fins and a greater pressure gradient improved mixing and heat transfer. They concluded also that the heat transfer was greatly affected by the fin dimensions. Maveety and Jung [6] presented experimental and numerical results for heat transfer from pin-fin heat sinks cooled by air impingement. It was shown that by minimizing the overall heat sink thermal resistance instead of maximizing the heat transfer from the fins was a better design criterion to optimize fin arrays. Kim and Kuznetsov [7] numerically studied the optimization of pin-fin heat sinks in a jet impinging channel. It was suggested that a thin pin-fin heat sink should be designed to have high porosity, while a thick pin-fin heat sink should have relatively low porosity. Park et al. [8] numerically investigated the optimum design of a fan-driven 7×7 pin-fin heat sink which minimized the thermal resistance and the pressure drop. The fin width and the fin height were found to be the dominant design variables, while the influence of the fan-to-heat sink distance on the thermal resistance and the pressure drop was comparatively small.

Only a limited amount of work is available to investigate the performance of plate-fin heat sinks with impingement cooling. Sathe and Sammakia [9] studied the optimized performance of the plate-fin heat sink under a rectangular impinging jet. The results showed that by cutting the fins located under the impingement zone reduced the pressure drop without sacrificing the heat transfer. Bhopte et al. [10] used a commercial package to explore the heat transfer of a plate-fin heat sink under impinging air cooling. The Nusselt was found to be dependent on the Reynolds number, the Rayleigh number, the nozzle diameter, the impingement distance and the heat sink geometry.

The infrared thermography technique utilizes the radiant exitance in the infrared spectral band from measured objects to measure temperature. It is non-intrusive, applicable remotely and suitable for measurement of a large area, and can also serve to record data for subsequent storage and processing with a computer. Meinders et al. [11] applied both infrared thermography and liquid crystal thermography to investigate local convective heat transfer from cubes in tunnel flow; these methods exhibited satisfactory consistency. Meinders and Hanjalic [12] investigated the heat transfer coefficient of an array of cubic objects in turbulent tunnel flow by measuring the surface temperature with infrared thermography; they also used Laser Doppler Anemometry to measure the velocity distribution. Ay et al. [13] used an infrared thermography camera to observe the surface temperature of a plate-finned-tube heat exchanger and calculated the local heat transfer coefficient.

From the previous literature reviews, the impinging jet cooling combined with a heat sink is generally applicable for cooling of electronic devices. Due to the complexity of the thermal-fluid characteristics in this approach, a greater understanding of the fluid flow and heat transfer

should be achieved in order to enhance the performance of this cooling technique. The objective of this paper is to investigate experimentally the thermal performance of plate-fin heat sinks under confined impinging jet conditions. The influences of the Reynolds number, the impingement distance, the width and the height of the fins on the performance are discussed.

2. Experimental apparatus and data reduction

The experimental equipment, shown schematically in Fig. 1, consists of an infrared thermography system, a confined impinging jet system, heat sinks, a heating element and thermal insulated device, and a system to measure flow rate and temperature. The infrared thermal imaging system (FLIR systems' ThermaCAM SC500 camera and AGEMA Research software) has a range of temperature measurement from −20 °C to 1500 °C with ±2% accuracy. The IR camera utilizes a 320 × 240 pixels uncooled focal plane array detector operated over the wavelength range from 7.5 μm to 13 μm. The field of view is 24° × 18°, the instantaneous field of view is 1.3 mrad, and the thermal sensitivity is 0.1 °C at 30 °C. Images is transferred to a computer in almost real time and stored therein for further analysis [14,15].

The confined impinging jet system consists of a nozzle, confining plates, orifice meters and a blower. To investigate the thermal performance of the heat sink subjected to confined impingement cooling, the confining plates are attached to the edges of the nozzle exit and the heat sink base. The cooling air is sucked by the blower, collected by the casing and sent to the orifice meter to measure its flow rate. A thermocouple is embedded into the nozzle in order to measure the jet temperature. The impinging jet ejects steadily from the nozzle to the heated heat sink and removes heat constantly. A nozzle of diameter (D) 8 mm is used and the impingement distance (Y) between the nozzle and the tip of the fins is set as 96 mm for reference.

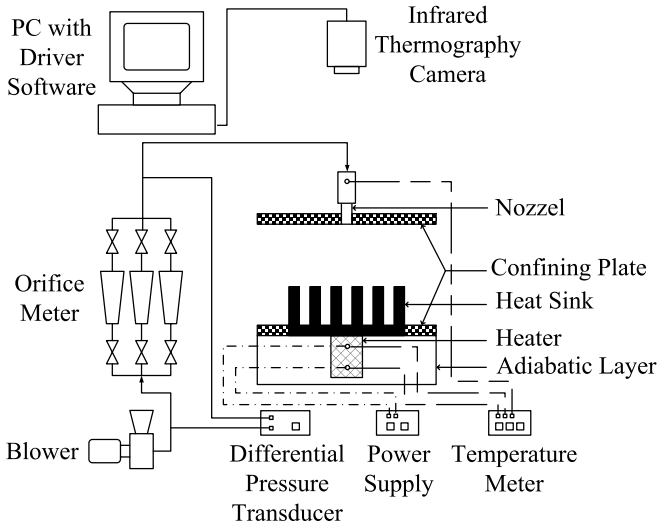

Fig. 1. The schematic diagram of the experimental apparatus.

The plate-fin heat sinks are designed as an array of 6 × 2 with a cut-off passage in the x-direction. The material of the heat sinks is selected as aluminum alloy 6061 and the surfaces are coated with a flat black paint that has a radiation emissivity of 0.96 to increase the accuracy of temperature measurement. The length and width (L) of the base of the heat sinks are 80 mm and the thickness (b) is 8 mm. The height and width of the fins are varied as experimental parameters. There are 25 heat sink models in this study with 5 fin widths and 5 fin heights as shown in Table 1 and Fig. 2. The heat transfer area of the plate-fin heat sink is given by $A_t = L^2 + nH(2W + L - G)$.

The heating element is covered with the insulated material, except on the top where it is in contact with the heat sink. The heating power is supplied from a DC source. It is expressed as

$$Q = \frac{k_{al} A (T_l - T_u)}{d} \tag{1}$$

where k_{al} denotes the thermal conductivity of heating aluminum alloy 6061 and has a value 168 W/mK. T_u and T_l are the temperatures of the upper and lower thermocouples, respectively, installed in the heating element. A signifies the cross-sectional area of the heating element, and d

Table 1
The specifications of the plate-fin heat sinks

No.	W (mm)	G (mm)	H (mm)	A_t (mm^2)
1	6.5	8.2	30 ($H/L = 0.3750$)	36,928
2	($W/L = 0.08125$)	($G/L = 0.1025$)	35 ($H/L = 0.4375$)	42,016
3			40 ($H/L = 0.5000$)	47,104
4			45 ($H/L = 0.5625$)	52,192
5			50 ($H/L = 0.6250$)	57,280
6	8.0	6.4	30 ($H/L = 0.3750$)	38,656
7	($W/L = 0.10000$)	($G/L = 0.0800$)	35 ($H/L = 0.4375$)	44,032
8			40 ($H/L = 0.5000$)	49,408
9			45 ($H/L = 0.5625$)	54,784
10			50 ($H/L = 0.6250$)	60,160
11	9.5	4.6	30 ($H/L = 0.3750$)	40,384
12	($W/L = 0.11875$)	($G/L = 0.0575$)	35 ($H/L = 0.4375$)	46,048
13			40 ($H/L = 0.5000$)	51,712
14			45 ($H/L = 0.5625$)	57,376
15			50 ($H/L = 0.6250$)	63,040
16	11.0	2.8	30 ($H/L = 0.3750$)	42,112
17	($W/L = 0.13750$)	($G/L = 0.0350$)	35 ($H/L = 0.4375$)	48,064
18			40 ($H/L = 0.5000$)	54,016
19			45 ($H/L = 0.5625$)	59,968
20			50 ($H/L = 0.6250$)	65,920
21	12.5	1.0	30 ($H/L = 0.3750$)	43,840
22	($W/L = 0.15625$)	($G/L = 0.0125$)	35 ($H/L = 0.4375$)	50,080
23			40 ($H/L = 0.5000$)	56,320
24			45 ($H/L = 0.5625$)	62,560
25			50 ($H/L = 0.6250$)	68,800
	$L = 80$ mm, $b = 8$ mm			

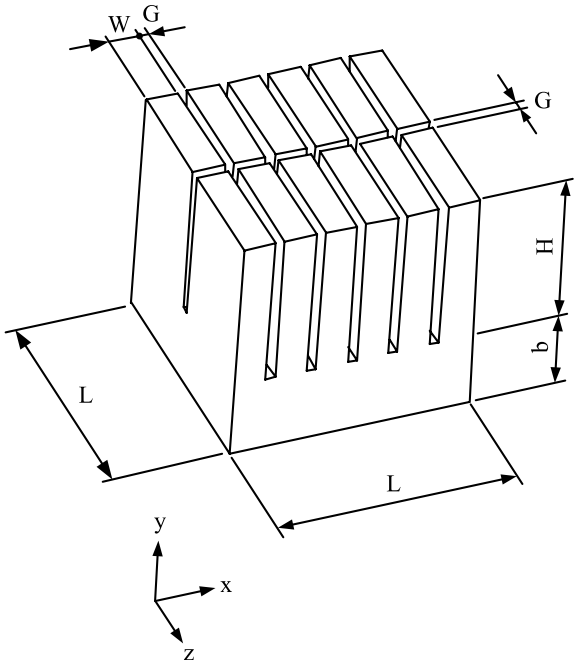

Fig. 2. The sketch of a plate-fin heat sink.

denotes the distance between the upper and lower thermocouples. The range of heating power in the experiments is 19.2–25.73 W. From our investigation of the influence of varying the heating power we conclude that it does not alter the thermal resistances over the range examined [16].

We use three orifice meters to cover the range of measurements 0.039–0.099 m^3/min, 0.059–0.189 m^3/min and 0.133–0.283 m^3/min. T-type thermocouples are used to measure temperatures of both the jet fluid and the heating element.

The experiments are performed and the temperature distributions obtained by the infrared thermography system are manipulated with a computer and associated software. We thereby obtain the average temperature of the base of the heat sink and evaluate the thermal performance.

The thermal resistance of heat sink is defined as

$$R_{\mathrm{th}} = \frac{T_{\mathrm{ave}} - T_{\infty}}{Q} = \frac{1}{UA_{\mathrm{t}}} \tag{2}$$

where T_{ave} is the average temperature of the base of the heat sink, T_{∞} is the temperature of the impinging jet, U is the overall heat transfer coefficient, and A_{t} is the heat transfer area which consists of the top of the base and the fins of the heat sink. This equation indicates that a larger heat transfer area or a higher overall heat transfer coefficient may lead to a smaller thermal resistance. In other words, more heat may be removed if the thermal resistance becomes smaller, so better thermal performance may be achieved. The Reynolds number of the impinging jet is calculated by

$$Re = \frac{VD}{\nu} \tag{3}$$

where V is jet velocity and ν is the kinematic viscosity of air.

The relative uncertainty of the thermal resistance is expressed as [17]

$$\frac{\delta R_{\mathrm{th}}}{R_{\mathrm{th}}} = \left\{ \left[\frac{\delta(T_{\mathrm{ave}} - T_{\infty})}{T_{\mathrm{ave}} - T_{\infty}} \right]^2 + \left(\frac{\delta Q}{Q} \right)^2 \right\}^{1/2} \tag{4}$$

The relative uncertainties of the heating power Q and the impinging Reynolds number Re are obtainable in similar ways. The maximum relative uncertainties of the thermal resistance, the heating power, and the Reynolds number for the experiments are estimated to be 14.3%, 7.1%, and 2%, respectively.

3. Results and discussion

The temperature of the plate-fin heat sink is measured by the infrared thermography technique in this paper; furthermore, the influences of various parameters on the thermal performance of the heat sink are investigated by evaluating the thermal resistance from the experimental results. The experimental parameters considered contain the Reynolds number, the impingement distance, the fin width and the fin height. The rangers of the parameters are described below:

1. Reynolds number: $Re = 5000$, 10,000, 15,000, 20,000 and 25,000.
2. Impingement distance: $Y = 32$, 64, 96, 128, 160, 192 and 224 mm ($Y/D = 4$, 8, 12, 16, 20, 24 and 28).
3. Fin width: $W = 6.5$, 8.0, 9.5, 11.0 and 12.5 mm ($W/L =$ 0.08125, 0.1, 0.11875, 0.1375 and 0.15625).
4. Fin height: $H = 30$, 35, 40, 45 and 50 mm ($H/L = 0.375$, 0.4375, 0.5, 0.5625 and 0.625).

3.1. The temperature distribution on the surface of the heat sink

Fig. 3 shows the temperature distribution of the top surface of the heat sink by infrared thermography under the conditions $Y/D = 12$, $W/L = 0.11875$, $H/L = 0.5625$, $Q = 21.66$ W, $Re = 15{,}000$. The temperature gradient indicates the direction of heat transfer in the heat sink to be outward from the inside and upward from the bottom because the heating element is in the center and contacts with a quarter of the heat sink bottom.

3.2. The influence of the Reynolds number on the thermal performance

The influence of the Reynolds number on the thermal performance is demonstrated in Fig. 4 for various fin widths with $Y/D = 12$ and $H/L = 0.5$. It is noted that the thermal resistance can be reduced effectively with the increase of the Reynolds number. The decreasing ratios of the thermal resistance with the Reynolds number for different fin widths are shown in Fig. 5. The decreasing ratios of the thermal resistance for the heat sink with fin

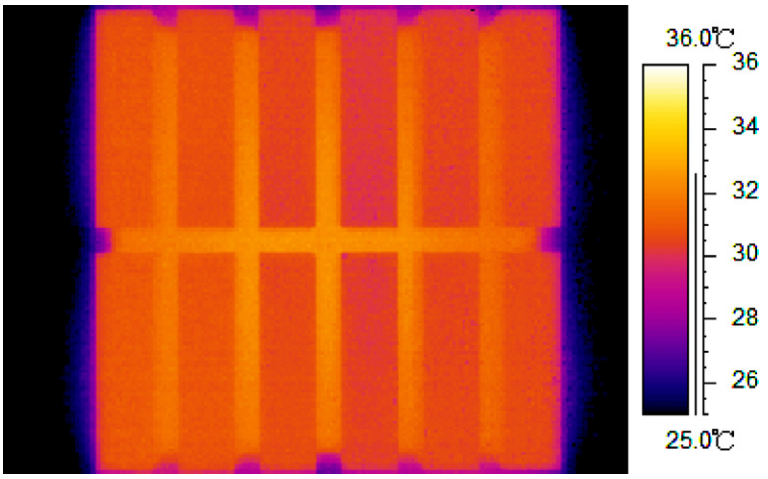

Fig. 3. The temperature distribution of a heat sink under the conditions $Y/D = 12$, $W/L = 0.11875$, $H/L = 0.5625$, $Q = 21.66$ W, $Re = 15{,}000$.

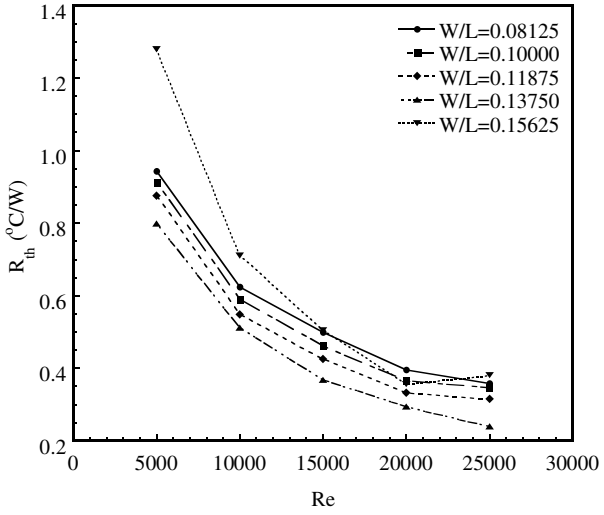

Fig. 4. The influence of the Reynolds number on the thermal resistance for various fin widths with $H/L = 0.5$ and $Y/D = 12$.

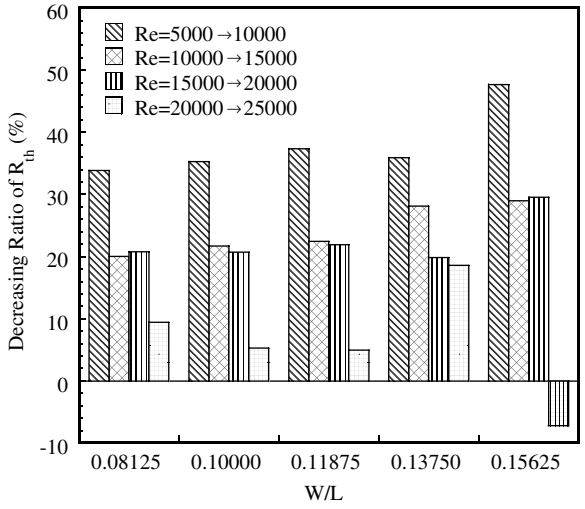

Fig. 5. The decreasing ratios of the thermal resistance with the Reynolds number for various fin widths with $H/L = 0.5$ and $Y/D = 12$.

width $W/L = 0.11875$ are 37.34%, 22.43%, 21.89% 4.94%, respectively, when the Reynolds number increases from 5000 to 10,000, 15,000, 20,000 and 25,000. The highest thermal resistance decreasing ratio occurs when the Reynolds number increases from 5000 to 10,000. The decreasing ratios are similar when the Reynolds number increases from 10,000 to 15,000 and from 15,000 to 20,000. Moreover, the decreasing ratio becomes apparently lower when the Reynolds number increases from 20,000 to 25,000. Generally speaking, the similar trend of the thermal resistance decreasing ratio is observed if the fin width of the heat sink varies. Thus, $Re = 20{,}000$ is the most effective value to apply for lowering the thermal resistance.

3.3. The influence of the impinging distance on the thermal performance

The variation of the impinging distance affects not only the velocity of the jet into the heat sink but also the impinging range of the jet within the heat sink. To investigate the influence of the impinging distance (Y/D) on the thermal resistance, the fin width and fin height of the heat sink are selected to be $W/L = 0.1$ and $H/L = 0.5$. The results are shown in Figs. 6 and 7. As shown in Fig. 6, the thermal resistance rises if the impinging distance Y/D is too long or too short, and an appropriate Y/D can cause the thermal resistance to reduce effectively. The results indicate that initially the thermal resistance decreases obviously with an increase of Y/D when the Reynolds number is 5000. The minimum thermal resistance is achieved at $Y/D = 16$. Afterward, the trend is reversed and the thermal resistance rises with increasing Y/D. This is because the impinging region of the jet is limited which declines the heat exchange between the jet and the heat sink if the impinging distance is too short. On the other hand, the jet may not be able to enter the inter-fin space effectively to remove heat if the impinging distance is too long. When the Reynolds number increases to 10,000 and 15,000, more jets are allowed to

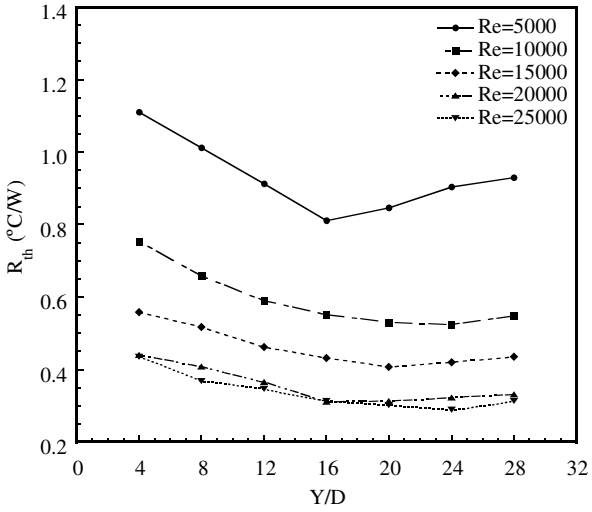

Fig. 6. The influence of the impinging distance on the thermal resistance with $W/L = 0.1$ and $H/L = 0.5$.

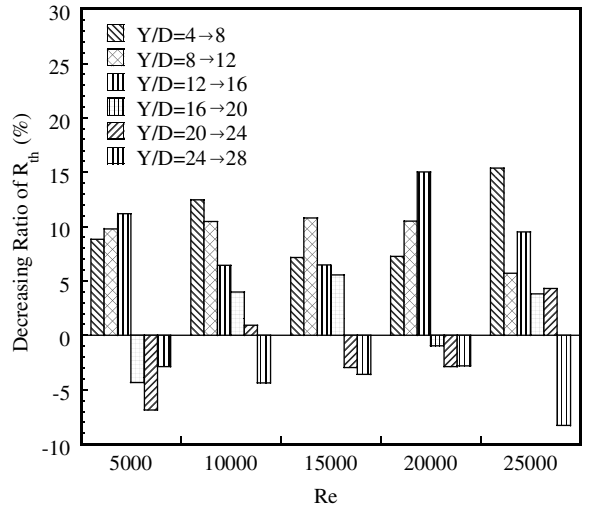

Fig. 7. The decreasing ratios of the thermal resistance with the impinging distance for various Reynolds numbers with $W/L = 0.1$ and $H/L = 0.5$.

flow into the inter-fin space to remove heat which results in sharply decreases of the thermal resistance for different Y/Ds. Additionally, the optimal Y/D is also lengthened, i.e. $Y/D = 20$. When the Reynolds number reaches 20,000 and 25,000, the influence of the impinging distance on the thermal resistance becomes obscure and the thermal performance is similar.

To sum up, the optimal impinging distance increases with increasing Reynolds number of the impinging jet. Besides, the improvement of the thermal resistance by the impinging distance is less significant for higher Reynolds numbers. Owing to the demand of compact size of electronic devices, increasing the impinging distance to improve the thermal resistance beyond a certain range seems to be impractical. Therefore, the optimal impinging distance is set to be $Y/D = 16$ in this study by considering the system size and the thermal performance.

3.4. The influence of the fin geometry on the thermal performance

The relationship between the fin width W and the inter-fin spacing G of the plate-fin heat sink considered can be calculated by $L = \frac{n}{2}W + \left(\frac{n}{2} - 1\right)G$, where L is the length of the base of the heat sink and n is the fin number. The influence of the fin width and the fin height on the thermal resistance are shown in Figs. 8 and 9 for $Y/D = 12$ and $Re = 5000$, 10,000, 25,000. The inter-fin spacing becomes larger when the fin width decreases. The flow can enter the heat sink more easily to facilitate the heat exchange between the heat sink and the jet that results in a higher overall heat transfer coefficient. However, the heat transfer area becomes smaller in this case that impedes the heat transfer. The results reveal that increasing the fin width

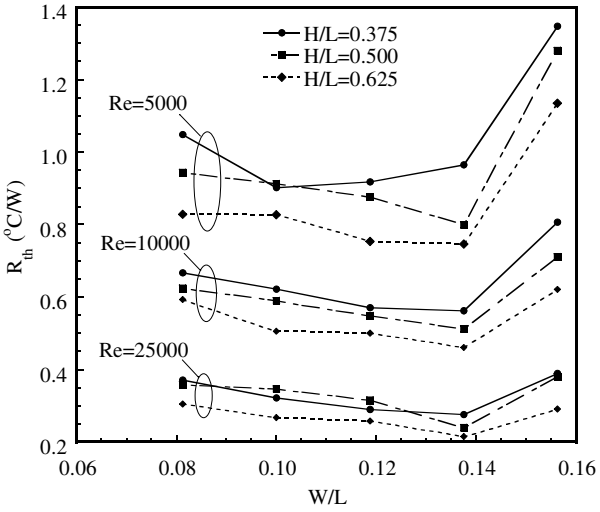

Fig. 8. The influence of the fin width on the thermal resistance for various fin heights with $Y/D = 12$.

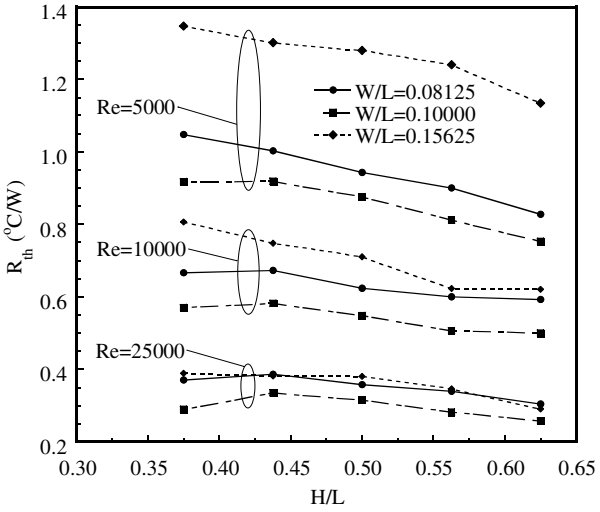

Fig. 9. The influence of the fin height on the thermal resistance for various fin widths with $Y/D = 12$.

can reduce the thermal resistance initially, but the thermal resistance may rise once the fin width is greater than a certain value. It is found that the lowest thermal resistance occurs at $W/L = 0.1$ when the Reynolds number is 5000 and the fin height is $H/L = 0.375$. The lowest thermal resistance is found at $W/L = 0.1375$ for all other experiment data. Thus, the optimal fin width in this study is selected as $W/L = 0.1375$.

Fig. 9 shows the effect of the fin height on the thermal resistance of the heat sink. The heat transfer areas of the heat sinks increase approximately 55% if the fin height increases from $H/L = 0.375$ to $H/L = 0.625$. The thermal resistance reduces significantly with increasing fin height at $Re = 5000$. It implies that the lack of fluid momentum to drive effective force convection at lower Reynolds number can be compensated by increasing the fin height to augment the heat transfer area. However, the influence of the fin height becomes insignificant if the Reynolds number rises up to 10,000 and 25,000, because the increased area locates on the tip of the heat sink where the temperature is low.

4. Conclusions

This study utilizes the infrared thermography technique to measure the thermal performance of the plate-fin heat sinks under confined impinging jet conditions at different Reynolds numbers, impingement distances, fin widths and fin heights. We conclude as follows from the experimental results.

1. The thermal resistance is influenced strongly by the Reynolds number of the impinging jet. To increase the Reynolds number can reduce the thermal resistance effectively. Moreover, the reduction of the thermal resistance decreases gradually with the increase of the Reynolds number. Thus, the improvement of the thermal resistance by increasing the Reynolds number has a limitation. By considering the decreasing rate of the thermal resistance, the optimal Reynolds number in this study is set to be 20,000.
2. The thermal resistance of the heat sink rises if the impinging distance is too short or too long. If the impinging distance is too short, the impinging region of the jet is limited which declines the heat exchange between the jet and the heat sink. Conversely, the jet may not be able to enter the inter-fin space effectively for cooling if the impinging distance is too long. Both situations cause the thermal resistance to decline. The optimal impinging distance increases with increasing Reynolds number of the impinging jet. Moreover, the improvement of the thermal resistance by increasing the impinging distance is less significant for higher Reynolds numbers. The suggested optimal impinging distance is $Y/D = 16$ in this study.
3. The increase of the fin width can reduce the thermal resistance effectively, but the thermal resistance may rise once the fin width is greater than a certain value. A heat sink with a wider fin width provides a larger area to increase the heat transfer between the heat sink and the impinging jet. However, an over-extended fin width restrains the inter-fin space and results in less fluid flow into the heat sink. Thus, the thermal resistance severely rises. The fin width $W/L = 0.13750$ is optimal for the most of the heat sinks and the Reynolds numbers conducted in this study.
4. Although increasing the fin height may increase the heat transfer area, the increased area locates on the tip of the heat sink where the temperature is low. Therefore, the effect of increasing the fin height on the thermal resistance is less effectively than that by increasing the fin width.

Acknowledgement

The authors would like to thank the National Science Council of the Republic of China for financially supporting this research under Contract No. NSC 93-2212-E-211-004.

References

[1] G. Ledezma, A.M. Morega, A. Bejan, Optimal spacing between pin fins with impinging flow, J. Heat Transfer 118 (1996) 570–577.
[2] S. Sathe, K.M. Kelkar, K.C. Karki, C. Tai, C. Lamb, S.V. Patankar, Numerical prediction of flow and heat transfer in an impingement heat sink, J. Electron. Packaging 119 (1997) 58–63.
[3] L.A. Brignoni, S.V. Garimella, Experimental optimization of confined air jet impingement on a pin fin heat sink, IEEE Trans. Compon. Pack. Technol. 22 (1999) 399–404.
[4] J.G. Maveety, J.F. Hendricks, A heat sink performance study considering material, geometry, nozzle placement, and Reynolds number with air impingement, J. Electron. Packaging 121 (1999) 156–161.
[5] J.G. Maveety, H.H. Jung, Design of an optimal pin-fin heat sink with air impingement cooling, Int. Commun. Heat Mass Transfer 27 (2000) 229–240.
[6] J.G. Maveety, H.H. Jung, Heat transfer from square pin-fin heat sinks using air impingement cooling, IEEE Trans. Compon. Pack. Technol. 25 (2002) 459–469.
[7] S.Y. Kim, A.V. Kuznetsov, Optimization of pin-fin heat sinks using anisotropic local thermal nonequilibrium porous model in a jet impinging channel, Numer. Heat Transfer, Part A 44 (2003) 771–787.
[8] K. Park, D.H. Choi, K.S. Lee, Numerical shape optimization for high performance of a heat sink with pin-fins, Numer. Heat Transfer, Part A 46 (2004) 909–927.
[9] S.B. Sathe, B.G. Sammakia, An analytical study of the optimized performance of an impingement heat sink, J. Electron. Packaging 126 (2004) 528–534.
[10] S. Bhopte, M.S. Alshuqairi, D. Agonafer, G. Refai-Ahmed, Mixed convection of impinging air cooling over heat sink in telecom system application, J. Electron. Packaging 126 (2004) 519–523.
[11] E.R. Meinders, T.H. van der Meer, K. Hanjalic, C.J.M. Lasance, Application of infrared thermography to the evaluation of local convective heat transfer on arrays of cubical protrusions, Int. J. Heat Fluid Flow 18 (1997) 152–159.
[12] E.R. Meinders, K. Hanjalic, Vortex structure and heat transfer in turbulent flow over a wall-mounted matrix of cubes, Int. J. Heat Fluid Flow 20 (1999) 255–267.

[13] H. Ay, J.Y. Jang, J.N. Yeh, Local heat transfer measurements of plate finned-tube heat exchangers by infrared thermography, Int. J. Heat Mass Transfer 45 (2002) 4069–4078.
[14] ThermaCAM SC500 operator's manual, FLIR Systems, Oregon, USA, 1999.
[15] ThermaCAM Researcher 2001 operating manual, FLIR Systems, Oregon, USA, 2000.
[16] H.Y. Li, K.Y. Chen, Thermal-fluid characteristics of pin-fin heat sinks cooled by impinging jet, J. Enhanc. Heat Transfer 12 (2005) 189–201.
[17] S.J. Kline, The purpose of uncertainty analysis, J. Fluids Eng. 107 (1985) 153–160.